Am J Physiol Cell Physiol
280: C110–C118, 2001.

Activation of MT_2 melatonin receptors in rat suprachiasmatic nucleus phase advances the circadian clock

AMANDA E. HUNT,[1] WALID M. AL-GHOUL,[2] MARTHA U. GILLETTE,[1,3] AND MARGARITA L. DUBOCOVICH[2]
[1]*Neuroscience Program and* [3]*Department of Cell and Structural Biology, University of Illinois at Urbana-Champaign, Urbana 61801; and* [2]*Department of Pharmacology and Biological Chemistry and Northwestern Drug Discovery Program, Northwestern University Medical School, Chicago, Illinois 60611*

Received 7 April 2000; accepted in final form 7 August 2000

Hunt, Amanda E., Walid M. Al-Ghoul, Martha U. Gillette, and Margarita L. Dubocovich. Activation of MT_2 melatonin receptors in rat suprachiasmatic nucleus phase advances the circadian clock. *Am J Physiol Cell Physiol* 280: C110–C118, 2001.—The aim of this study was to identify the melatonin receptor type(s) (MT_1 or MT_2) mediating circadian clock resetting by melatonin in the mammalian suprachiasmatic nucleus (SCN). Quantitative receptor autoradiography with 2-[^{125}I]iodomelatonin and in situ hybridization histochemistry, with either ^{33}P- or digoxigenin-labeled antisense MT_1 and MT_2 melatonin receptor mRNA oligonucleotide probes, revealed specific expression of both melatonin receptor types in the SCN of inbred Long-Evans rats. The melatonin receptor type mediating phase advances of the circadian rhythm of neuronal firing rate in the SCN slice was assessed using competitive melatonin receptor antagonists, the MT_1/MT_2 nonselective luzindole and the MT_2-selective 4-phenyl-2-propionamidotetraline (4P-PDOT). Luzindole and 4P-PDOT (1 nM-1 μM) did not affect circadian phase on their own; however, they blocked both the phase advances (~4 h) in the neuronal firing rate induced by melatonin (3 pM) at temporally distinct times of day [i.e., subjective dusk, circadian time (CT) 10; and dawn, CT 23], as well as the associated increases in protein kinase C activity. We conclude that melatonin mediates phase advances of the SCN circadian clock at both dusk and dawn via activation of MT_2 melatonin receptor signaling.

suprachiasmatic nucleus; brain slice electrophysiology; luzindole; 4-phenyl-2-propionamidotetraline; protein kinase C

THE BIOLOGICAL CLOCK located within the suprachiasmatic nucleus (SCN) times the near 24-h oscillations in neuroendocrine function (17). This clock signals production of the pineal hormone, melatonin, only at night. Thus the SCN clock generates the circadian rhythm of melatonin, ensuring that it is a neuroendocrine signal of darkness (16). However, melatonin can feed back on the clock to regulate its phase. The clock in the rat SCN brain slice is reset in response to melatonin at temporally distinct times, dusk and dawn (23, 24, 36). Nonselective melatonin receptor agonists, such as 2-iodomelatonin (23, 24), GR-196429 (6), and S-20098 (19), induce concentration-dependent phase advances when applied at dusk. In rodents, melatonin advances the phase of rhythms in wheel running activity at subjective dusk in vivo (3, 4, 14, 31). The melatonin-mediated phase advances in the rat SCN brain slice are blocked by treatment with pertussis toxin and specific inhibitors of protein kinase C (PKC) (24). Furthermore, melatonin activates PKC phosphotransferase activity at these windows of sensitivity but not at other times, and phorbol ester activators of PKC induce melatonin-like shifts. These data indicate that these phase shifts are mediated via activation of a G protein-coupled melatonin receptor signaling through a PKC pathway. This study probed the melatonin receptor type that mediates these effects on the circadian clock within the SCN.

In mammals, melatonin activates at least two distinct high-affinity membrane-bound receptors, the MT_1 and MT_2 receptors. These receptors show 60% homology at the amino acid level and are encoded by separate genes (32, 33, 35). The two melatonin receptors can be distinguished pharmacologically both in vivo and in vitro using subtype-selective melatonin receptor antagonists (10, 11, 13, 14). Acute inhibition of neuronal firing in the mouse SCN (22) and vascular vasoconstriction in the rat (8, 9) appear to be mediated through activation of the MT_1 melatonin receptor. By contrast, activation of the MT_2 melatonin receptor by melatonin inhibits dopamine release in the retina (13), mediates vasodilator responses in the rat vasculature (9), and phase advances circadian rhythms of wheel running activity in the C3H/HeN mouse (14). Although the expression of the MT_1 melatonin receptor correlates with a high density of 2-[^{125}I]iodomelatonin binding within the rodent brain (14, 22, 33), the expression pattern of the MT_2 melatonin receptor within the rat SCN has not yet been reported.

Address for reprint requests and other correspondence: A. E. Hunt, Dept. of Cell and Structural Biology, Univ. of Illinois, B107 CLSL, 601 S. Goodwin Ave., Urbana, IL 61801 (E-mail: a-hunt1@uiuc.edu).

The costs of publication of this article were defrayed in part by the payment of page charges. The article must therefore be hereby marked "*advertisement*" in accordance with 18 U.S.C. Section 1734 solely to indicate this fact.

The aim of this study was to assess the expression of both the MT_1 and MT_2 melatonin receptors and to identify the receptor mediating the action of melatonin on circadian clock resetting in the rat SCN. Using selective melatonin receptor antagonists, we demonstrated that melatonin acts via an MT_2, but not an MT_1, receptor to stimulate PKC activity and phase shift the circadian rhythm of neuronal firing activity in the rat suprachiasmatic circadian clock.

MATERIALS AND METHODS

Melatonin receptor nomenclature and classification. We used the official nomenclature for melatonin receptors approved by the Nomenclature Committee of the International Union of Pharmacology (11). The designations "mt_1" and "mt_2" correspond to those of the recombinant melatonin receptors previously known as Mel_{1a} (33) and Mel_{1b} (32), respectively. These receptors should be referred to in upper case, i.e., MT_1 and MT_2, to reflect the identification of their molecular structure and the pharmacological characterization of their function in native tissues (9, 13, 14, 40). MT_3 refers to the pharmacologically defined melatonin receptor, with yet unknown molecular structure, previously referred to as ML_2 (10).

Drugs and chemicals. Luzindole was synthesized by Dr. Mike Flaugh at Eli Lilly (Indianapolis, IN). 4-Phenyl-2-propionamidotetraline (4P-PDOT) was obtained from Tocris Cookson (Ballwin, MO). Melatonin was obtained from Sigma (St. Louis, MO).

Preparation of frozen brain slices. Male Long-Evans rats (8 wk old) from our colony, which have been inbred for more than 33 generations at the University of Illinois at Urbana-Champaign, were maintained in a 12:12-h light:dark cycle and killed by decapitation at zeitgeber time (ZT) 10. ZT 0 is defined as "lights on" in the rat colony; ZT 12 is "lights off". Circadian time (CT) is used to describe the state of the clock in the brain slice in constant conditions in vitro, using "lights on" as a reference point for CT 0. Brains were dissected, embedded in OCT compound, an embedding medium for frozen tissue specimens (Ted Pella, Reading, PA), and kept frozen at −80°C until sectioning. Coronal sections for receptor autoradiography (20 μm) or in situ hybridization (30 μm) were cut on a Reichert-Jung cryostat (Leica, Deerfield, IL) and mounted on either gelatin-coated or silane-coated slides, respectively. Rostro-caudal brain sections containing the SCN were successively placed on a series of nine slides so that sequential sections through the whole SCN could be analyzed. Slides were kept at −80°C until used.

Preparation of fixed brain slices. At ZT 10 on the day of fixation, animals were anesthetized with pentobarbital sodium (75–150 mg/kg) and perfused via the left ventricle with 50 ml phosphate-buffered saline (PBS) at room temperature. This perfusion was followed by 500 ml of freshly made paraformaldehyde solution (4%) in PBS. Brains were removed rapidly and postfixed in the same fixative solution for 24 h at 4°C. Brains were allowed to equilibrate in PBS that contained 20% sucrose at 4°C and were then sectioned in 30-μm thick sections on a Reichert-Jung cryostat.

Receptor autoradiography. Brain sections were processed for receptor autoradiography as previously described (14). Briefly, slide-mounted sections were air dried, preincubated with Tris-Ca^{2+} buffer (50 mM Tris·HCl and 4 mM $CaCl_2$, pH 7.4) for 30 min, and incubated with a saturating concentration of 2-[^{125}I]iodomelatonin (200 pM) for 1 h at 25°C in the absence and presence of melatonin (1 μM) to evaluate total and nonspecific binding, respectively. Sections were then rinsed twice for 5 min in Tris-Ca^{2+} buffer followed by a rapid rinse in ice-cold distilled water. Labeled sections were dried and exposed to Kodak Biomax MR scientific imaging film for 7 days. Films were developed in a film processor (Medical Film Processor QX-70, Konica). Optical densities were measured with a computer-based image analysis system (Bioquant System IV; R & M Biometrics, Nashville, TN) using ^{14}C standards calibrated for use with ^{125}I as described previously (26, 34).

In situ hybridization. Serial coronal rat brain sections were processed for isotopic or nonisotopic in situ hybridization using ^{33}P- or digoxigenin (DIG)-labeled oligonucleotide probes, respectively. Selective antisense and sense oligonucleotide probes corresponding to regions of the MT_1 and MT_2 melatonin receptor mRNA that had little homology to the heterologous (i.e., MT_2 and MT_1, respectively) sequences and with other published nucleotide sequences were chosen on the basis of guanine/cyclase content content and GenBank blast comparisons (2). Antisense oligonucleotide probes 100% complementary to rat melatonin receptor cDNA and their corresponding sense probes were used. The MT_1 antisense oligonucleotide probe (GGGGTCGTACTGGAGAGTTCCGGTTTGCAGG, 31 mer) is complementary to bases 108–138 of the partial rat MT_1 melatonin receptor cDNA sequence (GenBank accession no. U14409), and the MT_2 antisense oligonucleotide probe (CGGGTCATATTCTAGAGACCCCACAAAGAAA, 31 mer) is complementary to bases 111–141 of the partial rat MT_2 melatonin receptor cDNA sequence (GenBank accession no. U28218). Oligonucleotide probes were prepared at the Biotechnology Center of Northwestern University (Chicago, IL). For isotopic in situ hybridization, oligonucleotide probes were labeled with [α-^{33}P]dATP (Amersham Pharmacia Biotech, Piscataway, NJ) using terminal transferase (Roche Molecular Biochemicals, Indianapolis, IN) and purified using Nick columns (Amersham Pharmacia Biotech). For nonisotopic in situ hybridization, oligonucleotide probes were 3′ tailed with DIG-11-dUTP using the DIG-oligonucleotide tailing kit (Roche Molecular Biochemicals), according to manufacturer's instructions as previously described (14). Brain sections were hybridized with ^{33}P- or DIG-labeled oligoprobes following methods previously reported (14, 27). The hybridization signal generated by ^{33}P-labeled probes was detected by film autoradiography using Kodak Biomax MR scientific imaging film for 4 wk. Films were developed in a film processor (Medical Film Processor QX-70, Konica). The hybridization signal generated by DIG-labeled probes was detected using alkaline phosphatase-conjugated anti-DIG IgG (Roche Molecular Biochemicals), followed by chromagen 5-bromo-4-chloro-3-indolylphosphate-*p*-toluidine salt/nitro blue tetrazolium (Vector Labs, Burlingame, CA) in the presence of 1 mM levamisole.

The selectivity of the MT_1 and MT_2 oligonucleotide probes used to hybridize to target mRNAs was assessed by direct hybridization of corresponding labeled sense probes (0.5 pmol/100 μl) and by competition of the MT_1 and MT_2 oligonucleotide labeled antisense probes (0.5 pmol/100 μl) with 100 times the excess of their corresponding homologous or heterologous sense oligonucleotide probes. Toward this end, each DIG- or ^{33}P-labeled antisense oligonucleotide probe (MT_1 or MT_2) was hybridized to tissue sections under three experimental conditions. First, each labeled antisense probe was hybridized alone to determine the total hybridization signal. Second, each labeled probe was hybridized in the presence of 100 times the excess of nonlabeled heterologous sense probe of the other receptor to block cross hybridization. Third, hybridization was carried out in the presence of 100

times the excess of nonlabeled homologous sense probes to determine the extent of nonspecific hybridization.

Animals and brain slice preparation. Male Long-Evans rats (6- to 10-wk old) were used. Rats were removed from the colony and quickly decapitated during the lights on period only, usually around ZT 5–7. A 500-μM coronal brain slice that contained the paired SCN was prepared within 5 min and placed at the interface of a Hatton-style brain slice chamber (20). Slices were continuously perifused with Earle's balanced salt solution (EBSS; Life Technologies, Grand Island, NY) supplemented with 24.6 mM glucose, 26.2 mM sodium bicarbonate, and 5 mg/l gentamicin and saturated with 95% O_2–5% CO_2 at 37°C (final pH 7.4). Slices were under constant illumination and were allowed to equilibrate at least 2 h before any experimental paradigms were initiated.

Electrophysiology recordings and data analysis. The extracellular single unit activity from SCN neurons was sampled throughout the nucleus with a glass microelectrode filled with 5 M NaCl and positioned by a hydraulic microdrive, as previously described (30). Every cell with a signal-to-noise ratio of at least 2:1 that was encountered was recorded, the average being 4–6 cells per hour. Each cell was monitored for 4 min, the action potentials were grouped into 10-s bins, and the mean firing rate was calculated for each cell. Data were collected using customized LabVIEW software (National Instruments, Austin, TX). Mean firing rates were grouped into 2-h bins and then smoothed by plotting the data as 15-min running averages. The time-of-peak was visually determined and compared with the time-of-peak of untreated control slices (peak = CT 7 ± 0.25, $n = 4$), which is coincident with the peak in vehicle-treated controls (24). Under these conditions, the SCN continues to generate stable circadian rhythms of neuronal activity that peak near CT 7 for up to 3 days (30).

Experimental treatments. Melatonin (1 μl) was applied directly to the SCN using the microdrop technique (25). For microdrop treatments, perifusion of the slice was stopped and a 1-μl droplet that contained melatonin at appropriate concentrations was applied to the SCN. Treatment was terminated by washing the reagent off the slice with a stream of fresh EBSS and continuing perifusion. Antagonists were administered by static bath application. The experimenter was blind to the identity of the antagonists being tested. For static bath treatments, perifusion of the slice was stopped at specified times, and the medium in the chamber was quickly removed and manually replaced with media that contained appropriate concentrations of vehicle or antagonists for 1 h. Static bath treatment was terminated by replacing the medium with fresh EBSS and resuming perifusion. For combination static bath/microdrop treatments, the antagonist being tested was bath applied to the slice for 25 min before a 1-μl microdrop that contained 3 pM melatonin was applied. After 10 min, the slice was washed off with EBSS that contained the antagonist, and the static bath incubation was continued for an additional 25 min. Media was replaced with fresh EBSS and perifusion resumed. Melatonin was dissolved to 1 mM in 95% ethanol and further diluted in EBSS. 4P-PDOT and luzindole were dissolved to 10 mM in 95% ethanol and diluted to 1 mM in 50% ethanol. Further serial dilutions were performed in EBSS. The maximal concentration of ethanol used in these experiments (0.001%) does not alter SCN phase (24).

PKC activity assays. PKC activity assays in SCN slices were performed as previously described (24). Briefly, brain slices surgically reduced to contain the SCN and optic chiasm were incubated with antagonists (bath application, 25 min) and/or melatonin the same as for recording experiments, except that melatonin was applied as a microdrop for 1 min, because this has been shown to produce maximal activation of PKC (24). Slices were then quickly frozen on dry ice. Slices were thawed in dilution buffer and phosphotransferase activity was evaluated using a PKC assay kit (Upstate Biotechnology, Lake Placid, NY). Activity was based on incorporation of [γ-^{32}P]ATP (DuPont-NEN, Boston, MA) into a synthetic substrate peptide corresponding to amino acid residues 4–14 of myelin basic protein, in the absence of lipids. The protein content of each slice was determined using the method of Bradford (7), and the specific activity was expressed as counts per minute per microgram of protein.

RESULTS

Melatonin receptor expression in rat SCN. Receptor autoradiography with the radioligand 2-[^{125}I]iodomelatonin revealed robust specific binding in the SCN at CT 10 (Fig. 1*A*). The specific binding of a saturating concentration of 2-[^{125}I]iodomelatonin (200 pM) defined with melatonin (1 μM) was 17.2 ± 0.4 fmol/mg protein

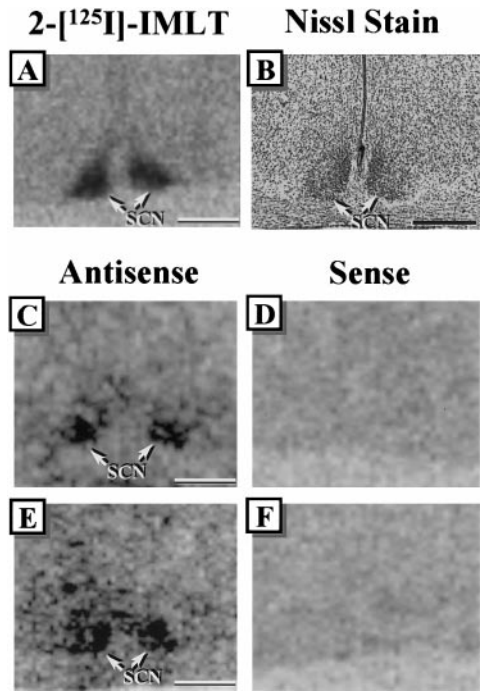

Fig. 1. Melatonin receptor binding and mRNA expression in the rat suprachiasmatic nucleus (SCN). *A*: a representative autoradiogram of 2-[^{125}I]iodomelatonin (2-[^{125}I]-IMLT) binding to the rat SCN. To evaluate total binding (*A*), frozen coronal sections encompassing the SCN were incubated with 2-[^{125}I]iodomelatonin (200 pM). Nonspecific binding was determined by coincubation with melatonin (1 μM) and revealed no binding (data not shown). *B*: Nissl stain of a coronal section comprising the SCN at similar magnification as *A* and *C–F*. *C* and *E*: hybridization signal of ^{33}P-labeled antisense oligonucleotide probes for the MT_1 (*C*) and MT_2 (*E*) melatonin receptor mRNA to frozen coronal sections containing the SCN. Nonspecific hybridization to frozen coronal sections encompassing the SCN was determined by in situ hybridization autoradiography utilizing ^{33}P-labeled antisense MT_1 and MT_2 oligonucleotide probes with 100-fold excess of the homologous sense oligonucleotide probe (*D* and *F*). By contrast, hybridization of ^{33}P-labeled antisense MT_1 and MT_2 oligonucleotide probes were not competed by the corresponding heterologous sense probe (see Table 1). Scale bars for *A–C* and *E*, 0.5 mm.

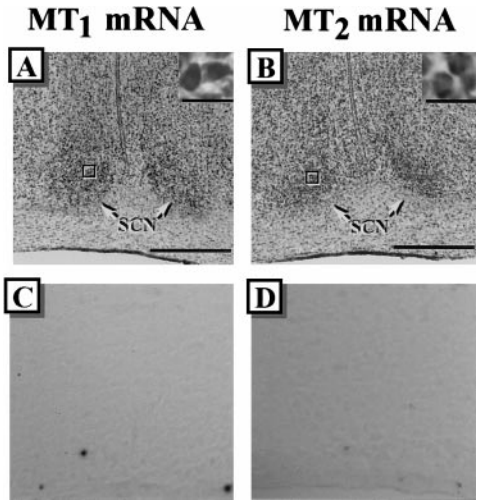

Fig. 2. MT_1 and MT_2 melatonin receptor mRNA expression in the rat SCN. *A–D*: micrographs of the hybridization signal for digoxigenin (DIG)-labeled MT_1 and MT_2 antisense (*A–B*) and sense (*C–D*) oligonucleotide probes to rat SCN frozen sections. The hybridization signal was discretely localized throughout the SCN with both MT_1 antisense probe (*A*) and MT_2 antisense probe (*B*). No hybridization was detected with MT_1 and MT_2 sense probes (*C* and *D*, respectively). Scale bar, 0.5 mm. *Insets*: SCN cells taken from regions delineated by white squares in *A* and *B* at high magnification, demonstrating that hybridization to mRNA was restricted to the cytoplasm. Scale bar, 20 μm.

($n = 3$). Nissl stain (Fig. 1*B*) of adjacent sections revealed almost complete overlap of 2-[^{125}I]iodomelatonin binding with the SCN.

Antisense oligonucleotide probes complementary to target sequences of the rat MT_1 and MT_2 melatonin receptor cDNA labeled with either ^{33}P (Fig. 1, *C* and *E*) or DIG (Fig. 2, *A* and *B*) showed specific hybridization to frozen sections of rat SCN. Hybridization of the MT_1 and MT_2 ^{33}P-labeled probes was competed by 100-fold excess of the corresponding unlabeled homologous sense probe (Table 1; Fig. 1, *D* and *F*). By contrast, 100 times excess of the corresponding unlabeled sense heterologous probe did not compete for either the MT_1 or MT_2 ^{33}P-labeled probes (Table 1). Furthermore, no hybridization of the MT_1 and MT_2 DIG-labeled sense probes was observed in sections that contained the SCN (Fig. 2, *C* and *D*). Cellular labeling was observed throughout the SCN with both MT_1 and MT_2 oligonucleotide probes. At higher magnification, we observed that mRNA hybridization of both the MT_1 and MT_2 antisense DIG-labeled oligonucleotide probes localized to the cytoplasmatic region of SCN cells (Fig. 2, *A* and *B*, *insets*). Generally, labeled cells had neuronlike morphology characterized by pear-shaped cell bodies with evidence of neuronal processes. However, whether labeling was present in glial cells could not be determined.

Figure 3, *A* and *C*, shows hybridization of DIG-labeled MT_1 and MT_2 melatonin receptor antisense

Table 1. *Selective hybridization of ^{33}P-labeled antisense oligonucleotide probes to MT_1 and MT_2 mRNA in rat SCN*

Unlabeled Sense Probe	^{33}P-Labeled Antisense Probe	
	MT_1	MT_2
None	8.6 ± 1.4	9.3 ± 2.6
Homologous (MT_1 or MT_2)	3.2 ± 0.9*	1.2 ± 0.9*
Heterologous (MT_2 or MT_1)	6.8 ± 1.3†	9.2 ± 2.0†

Data represent optical density measurements (means ± SE, $n = 6$) of hybridization signal of ^{33}P-labeled antisense oligonucleotide probes for the MT_1 and MT_2 melatonin receptor mRNA to frozen brain coronal sections containing the suprachiasmatic nucleus (SCN), as shown in Fig. 1, *C–F*. The specificity of the hybridization signal to frozen coronal sections encompassing the SCN was determined by in situ hybridization autoradiography utilizing ^{33}P-labeled antisense MT_1 and MT_2 oligonucleotide probes with 100-fold excess of either homologous or heterologous sense oligonucleotide probes. *$P < 0.05$ compared with hybridization with ^{33}P-antisense; †$P < 0.05$ compared with competition of homologous probe for ^{33}P-antisense hybridization.

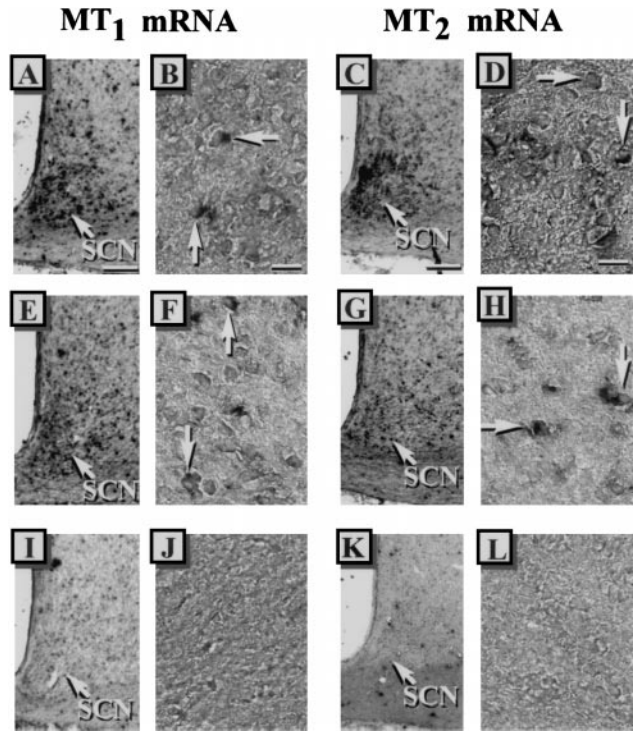

Fig. 3. Selective hybridization of DIG-labeled oligonucleotide probes reveals MT_1-expressing cells in the ventral SCN and MT_2-expressing cells in the ventromedial crescent. The micrographs show hybridization of DIG-labeled MT_1 (*A*, *B*, *E*, *F*, *I*, and *J*) and MT_2 (*C*, *D*, *G*, *H*, *K*, and *L*) melatonin receptor mRNA antisense oligonucleotide probes to perfused-fixed coronal sections encompassing the SCN under the following experimental conditions. *A–D*: DIG-labeled MT_1 or MT_2 probes alone; *E–H*: DIG-labeled MT_1 and MT_2 probes in the presence of 100-fold excess heterologous unlabeled MT_2 (*E* and *F*) and MT_1 (*G* and *H*) sense oligoprobes; *I–L*: DIG-labeled MT_1 and MT_2 probes in the presence of 100-fold excess homologous unlabeled MT_1 (*I* and *J*) and MT_2 (*K* and *L*) sense oligoprobes. Scale bars, 200 μm (*A*, *C*, *E*, *G*, *I*, and *K*). High magnification of single cells (*B*, *D*, *F*, *H*, *J*, and *L*) shows hybridization of DIG-labeled MT_1 and MT_2 probes in the absence (*B* and *D*, respectively) or in the presence (*F* and *H*, respectively) of excess unlabeled sense heterologous probes. Note the ringed pattern of the label, which indicates cytoplasmatic localization. No signal was evident when DIG-labeled MT_1 and MT_2 antisense probes were tested in the presence of corresponding homologous probes (*J* and *L*, respectively). Scale bars, 20 μm (*B*, *D*, *F*, *H*, and *L*).

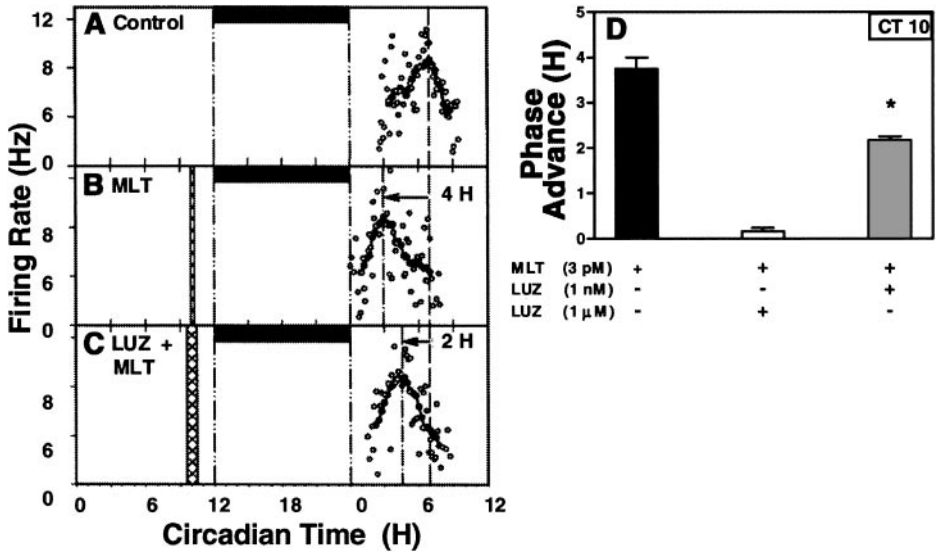

Fig. 4. Luzindole (LUZ) antagonized the melatonin (MLT)-induced phase advance of the circadian rhythm of neuronal firing activity when applied to the rat SCN at circadian time (CT) 10. *A*: the peak in SCN neuronal firing rate occurs near CT 7 in both untreated brain slices and in vehicle-treated controls. *B*: a microdrop (1 μl) of melatonin (3 pM) applied to the SCN at CT 10 induced a 4-h phase advance. *C*: the nonselective melatonin receptor antagonist luzindole (1 nM) bath applied to the SCN before a melatonin (3 pM) microdrop attenuated the 4-h phase advance. ○, the firing rate of individual cells. The dark gray horizontal bar represents subjective night. The vertical dashed lines represent peak times. Crosshatched bars indicate time of treatment. *D*: summary of the data. Results are plotted as means ± SE ($n = 3$ in each group). *$P < 0.05$ compared with melatonin.

oligonucleotide probes, respectively, to the rat SCN in fixed coronal sections. The hybridization signal observed with antisense DIG-labeled MT_1 (Fig. 3*A*) or MT_2 probes (Fig. 3*C*) was not altered in the presence of a 100-fold excess of nonlabeled heterologous sense MT_1 (Fig. 3*E*) or MT_2 (Fig. 3*G*) oligonucleotide probe, respectively. By contrast, a 100-fold excess of nonlabeled homologous sense MT_1 (Fig. 3*I*) or MT_2 (Fig. 3*K*) oligonucleotide probe completely blocked hybridization of the corresponding labeled probe. At higher magnification, we observed cellular hybridization of both the MT_1 and MT_2 antisense DIG-labeled oligonucleotide probes in the absence (Fig. 3, *B* and *D*) and presence (Fig. 3, *F* and *H*) of the corresponding sense heterologous nonlabeled probes. The hybridization signal localized to the cytoplasmatic rim of the cells, sometimes exhibiting a donut-shaped profile of labeling. The sense homologous nonlabeled probes blocked hybridization of the MT_1 (Fig. 3*J*) and MT_2 (3*L*) antisense DIG-labeled probes to SCN cells, respectively. Together, these results confirm the specificity of the antisense MT_1 and MT_2 oligonucleotide probes, labeled with either ^{33}P or DIG, for their mRNA targets as well as the lack of cross hybridization.

MT_2 melatonin receptor-mediated phase shifts of neuronal firing rate. The peak in neuronal electrical activity in control SCN slices occurred at CT 7.00 ± 0.25 ($n = 4$; Fig. 4*A*). Exposure of the SCN to melatonin (0.1–3 pM) delivered by microdrops reset the circadian clock in a concentration-dependent manner, reaching a plateau at 1 nM. Melatonin (3 pM) applied by microdrop to the SCN at CT 10 induced a nearly 4-h phase advance ($Ø_A$) in the peak of firing rate (Fig. 4, *B* and *D*; $Ø_A = 3.83 \pm 0.29$ h, $n = 3$). This is of similar magnitude to the phase shift induced by bath application (24, 36).

To evaluate the nature of the receptor mediating the melatonin-induced phase shift at subjective dusk (CT 10), we examined the interactions of melatonin with two melatonin receptor-specific competitive antagonists, luzindole and 4P-PDOT (13, 14). Bath application of the nonselective melatonin receptor antagonist luzindole (1 μM) at CT 10 did not affect the time-of-peak of electrical activity (data not shown; $Ø_A = 0.17 \pm 0.14$ h, $n = 3$). However, a 1,000-fold lower concentration significantly reduced the phase advance induced by 3 pM melatonin (Fig. 4, *C* and *D*; $Ø_A = 2.17 \pm 0.14$ h, $n = 3$; $P < 0.001$, Student's *t*-test), whereas a 1-μM treatment completely blocked the melatonin phase advance ($Ø_A = 0.25 \pm 0.25$, $n = 3$) (Fig. 4*D*). Next, the phase-shifting effect of 3 pM melatonin was examined in the presence of increasing concentrations of the selective and competitive MT_2 melatonin receptor antagonist, 4P-PDOT. Bath application of 4P-PDOT (1 μM) alone to the SCN did not affect the time-of-peak of electrical activity (Fig. 5; $Ø_A = 0.08 \pm 0.52$ h, $n = 3$). At

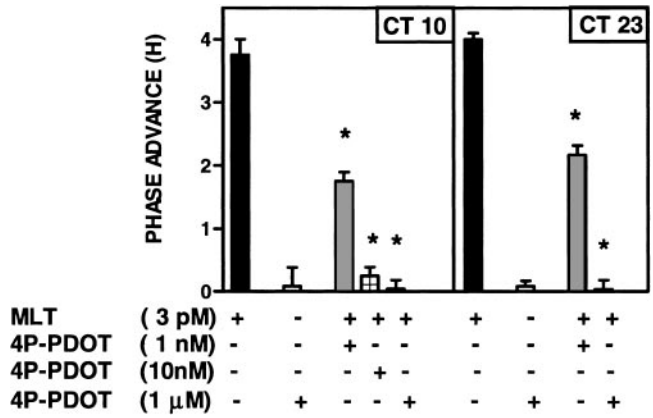

Fig. 5. The selective MT_2 melatonin receptor antagonist, 4-phenyl-2-propionamidotetraline (4P-PDOT), blocked melatonin-mediated phase advances of circadian rhythms of neuronal activity at both CT 10 and CT 23. Melatonin (3 pM) applied as a microdrop at CT 10 or CT 23 induced near 4-h phase advances. Bath application of 4P-PDOT (1 μM) did not induce a phase shift of its own. 4P-PDOT (1 nM, 10 nM, or 1 μM), bath applied to the slice before melatonin at CT 10 or CT 23, attenuated phase advances in a concentration-dependent manner. Results are plotted as means ± SE ($n = 3$ per group). *$P < 0.005$ compared with melatonin alone.

a concentration of 1 nM, 4P-PDOT attenuated the phase advance induced by 3 pM melatonin by 2 h ($Ø_A$ = 1.75 ± 0.25 h, n = 3; $P < 0.001$, Student's t-test). Higher concentrations of 4P-PDOT (10 nM and 1 μM) completely blocked the 4-h phase shift induced by 3 pM melatonin (Fig. 4; $Ø_A$ = 0.25 ± 0.25 h, n = 3; $Ø_A$ = 0.00 ± 0.25 h, n = 3, respectively).

To evaluate the melatonin receptor mediating phase shifts during subjective dawn, melatonin (3 pM) was applied by microdrop at CT 23. This induced a 3.83 ± 0.29-h (n = 3) phase advance, which is equivalent to that induced by bath applications at CT 23 (24). Bath application of the MT_2-selective melatonin receptor antagonist, 4P-PDOT, alone at 1 μM did not affect the time-of-peak of electrical activity ($Ø_A$ = 0.08 ± 0.14 h, n = 3; Fig. 5). At a concentration of 1 nM, 4P-PDOT significantly antagonized the phase advance induced by 3 pM melatonin ($Ø_A$ = 2.16 ± 0.29 h, n = 3; $P < 0.005$, Student's t-test), whereas a 1-μM concentration of 4P-PDOT completely blocked the 4-h phase advance induced by melatonin ($Ø_A$ = 0.0 ± 0.25 h, n = 3; $P < 0.001$, Student's t-test; Fig. 5). Therefore, these pharmacological data support the hypothesis that melatonin-induced phase advances at both dusk and dawn are mediated via activation of the MT_2 receptor.

MT_2 receptor activation stimulates PKC activity. To determine whether the melatonin receptor antagonists affected melatonin-induced PKC activation, a necessary step in the signal transduction pathway mediating phase shifts, enzyme assays were performed at CT 10. Application of 3 pM melatonin to the SCN brain slice doubled PKC phosphotransferase activity ($P < 0.05$, Student's t-test). Neither luzindole (1 μM) nor 4P-PDOT (1 μM) alone altered basal levels of PKC activity (Fig. 6). However, when luzindole or 4P-PDOT was applied before 3 pM melatonin, the rise in PKC activity was fully blocked (Fig. 6; $P = 0.132$, ANOVA on ranks). Thus the pharmacology of the receptor mediating the effect of melatonin on PKC activity is consistent with that mediating the effect of melatonin in clock resetting.

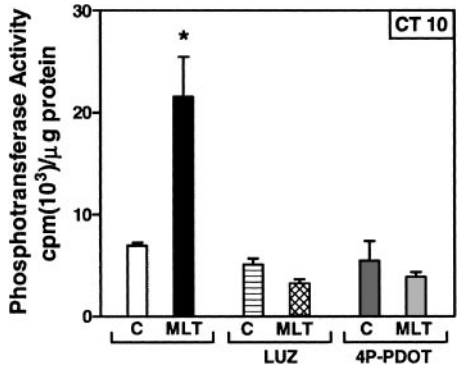

Fig. 6. Melatonin-mediated increases in protein kinase C (PKC) activity at CT 10 are antagonized by luzindole and 4P-PDOT. Melatonin application to the brain SCN slice increased PKC phosphotransferase activity twofold over basal levels at CT 10 ($P < 0.05$, Student's t-test). Luzindole (1 μM) or 4P-PDOT (1 μM) blocked the ability of melatonin to activate PKC ($P > 0.1$, ANOVA on ranks). Results are plotted as means ± SE (n = 3–5 per group). C, control. *$P < 0.05$ compared with control.

DISCUSSION

Here we report that in the rat SCN slice, the melatonin-mediated phase advances of circadian rhythms of neuronal firing rate and the increases in PKC activity are blocked by the selective and competitive MT_2 melatonin receptor antagonist, 4P-PDOT. Furthermore, we demonstrated expression of melatonin receptors in the rat SCN by autoradiography with 2-[^{125}I]iodomelatonin and by in situ hybridization using selective MT_1 and MT_2 melatonin receptor mRNA oligoprobes. We conclude that both the MT_1 and MT_2 melatonin receptors are expressed in the SCN of Long-Evans rats and that activation of MT_2 melatonin receptor signaling through PKC mediates the phase-shifting effects of melatonin on the circadian clock at both dusk and dawn.

The accumulation of biochemical, molecular, and functional evidence consistently suggests the presence of two melatonin receptors, the MT_1 and MT_2, in the mammalian SCN (14, 22, 32, 38, 40). Expression of both the MT_1 and MT_2 melatonin receptor mRNAs in the rat SCN was recently demonstrated by RT-PCR (38, 40). Our in situ hybridization histochemistry studies, using highly selective and specific oligonucleotide probes, revealed for the first time cellular expression of these two receptors within the rat SCN. Specific hybridization of the MT_1 and MT_2 probes within the ventral and ventromedial crescent of the SCN was previously reported in the C3H/HeN mouse (14). The signal from isotopic in situ hybridization with ^{33}P-labeled probes overlapped with SCN areas displaying specific 2[^{125}I]iodomelatonin binding sites. mRNA hybridization with both the MT_1 and MT_2 antisense probes was observed within the cytoplasmatic region of rat SCN cells that had neuronal morphology. This is in contrast to hybridization of MT_1 and MT_2 antisense DIG-labeled oligonucleotides to distinct cellular elements (MT_1: granule and basket cells; MT_2: Bergman glia and astrocytes) of the human cerebellar cortex (1). In this report, the specificity of labeling of each probe to the corresponding melatonin receptor was clearly demonstrated (1, 14). In the present study, we show concordance of labeling patterns with ^{33}P- and DIG-labeled probes and rigorously controlled for specificity by competition experiments. Thus our data reveal specific labeling of both MT_1 and MT_2 melatonin receptor mRNAs in the rat SCN and raise the question of the roles these receptors play in SCN function.

Activation of melatonin receptors in the SCN regulates incoming (e.g., light) and output circadian signals and has a direct effect on circadian clock timing (3, 5, 41). In mammals, including humans, melatonin-mediated phase shifts of the clock are restricted to two times of sensitivity, dusk and dawn (4, 21, 24). Specifically, in the rat SCN brain slice, bath-applied melatonin induces concentration-dependent advances of circadian rhythm of neuronal firing rate at both CT 10 and CT

23, with maximal phase shifts of 4 h (23, 24, 36). This model was used here to test the hypothesis that the effects of melatonin on circadian phase within the SCN are mediated through activation of a specific melatonin receptor.

The competitive melatonin receptor antagonist, luzindole, blocked both the melatonin-mediated phase advances of circadian rhythms of neuronal firing rate and the increases in PKC activity in the rat SCN. These results are compatible with activation of a G protein-coupled melatonin receptor (24, 36). Luzindole shows 15–25 times higher affinity for the MT_2 than the MT_1 melatonin receptor (13, 14, 29). In the mammalian retina, it antagonizes melatonin-mediated inhibition of dopamine release through activation of MT_2 melatonin receptors (13). Together, our data are consistent with melatonin acting at an MT_2 receptor to phase advance the clock at CT 10. These experiments, however, do not exclude participation of the MT_1 melatonin receptor in the phase shift induced by melatonin.

The case for the MT_2 receptor as mediator of the melatonin clock effect is strengthened by experiments with the specific and selective MT_2 melatonin receptor antagonist, 4P-PDOT (11). Exposure of the SCN slice to 4P-PDOT alone did not phase shift the clock, demonstrating that this analog is not acting as an agonist on melatonin or other G protein-coupled receptors within the SCN (12, 29). However, 4P-PDOT (1–10 nM, 1 μM) competitively antagonized melatonin-mediated phase advances of the circadian rhythm of neuronal firing rate in the rat SCN at two periods of melatonin sensitivity, CT 10 and CT 23. In vivo melatonin-mediated phase advances of circadian activity rhythms may occur primarily through activation of MT_2 melatonin receptors within the SCN, rather than in other areas of the circadian timing system, such as retina or intergeniculate nucleus (3, 4, 14, 28). The role of MT_2 melatonin receptors in the mammalian SCN in mediating phase advances of the biological clock is further supported by other findings. In the C57BL/6J mouse, targeted deletion of the MT_1 receptor did not alter the effect of melatonin on the clock; however, the melatonin-mediated acute inhibition of neuronal firing rate in the SCN was abolished (22). Furthermore, in the C3H/HeN mouse, in vivo administration of either luzindole or 4P-PDOT antagonized phase advances of circadian rhythms of wheel running activity mediated by melatonin at CT 10 (14). Together, these results suggest that selective MT_2 melatonin receptor agonists may mediate changes in clock phase and may have potential in the treatment of conditions characterized by alterations in circadian phase due to endogenous (e.g., delayed sleep phase syndrome and advanced sleep phase syndrome) or environmental (e.g., jet lag) causes (3).

In the rat SCN, phase shifting of circadian rhythms of neuronal firing rate appears to be mediated through activation of the MT_2 melatonin receptor signaling via activation of PKC. In support of this hypothesis, both luzindole and 4P-PDOT completely antagonized activation of PKC by melatonin. Both the MT_1 and MT_2 melatonin receptors were coupled to pertussis toxin-sensitive G proteins that mediate inhibition of forskolin-stimulated cAMP accumulation (18, 39). In the rat SCN, MT_2 melatonin receptors may signal through stimulation of phospholipase C (PLC) by G$\beta\gamma$-complexes generating inositol trisphosphate and diacylglycerol (DAG), which in turn activate PKC. In support of this hypothesis, direct activation of PKC with phorbol esters induces phase advances equivalent to those elicited by melatonin (24). Alternatively, MT_2 melatonin receptor-mediated stimulation of PKC in the SCN may involve a signal transduction mechanism as proposed for the MT_1 melatonin receptors (18), whereby G$\beta\gamma$-subunits activate phospholipase Cβ subsequent to $PGF_{2\alpha}$ stimulation. The aggregate data suggest that the MT_2 receptor couples to a pertussis toxin-sensitive G protein that activates PLC and DAG-mediated PKC activation.

In the Siberian hamster, a melatonin receptor other than the MT_2 appears to mediate phase shifting of circadian rhythms. This species expresses only the MT_1 receptor, naturally lacking MT_2 receptors, yet melatonin still phase advances the clock in vivo and in vitro (42). Species difference may account for this discrepancy. However, it is possible that the lack of functional MT_2 receptors may have altered the function of the MT_1 melatonin receptor, unmasking the contribution of this receptor to the phase shift. Alternatively, one may propose that the phase shifts induced by melatonin are mediated through activation of an MT_2 melatonin receptor isoform or splice variant not yet discovered.

What are the physiological roles of the MT_1 and MT_2 melatonin receptors within the SCN? The MT_1 contributes to the reversible decrease in firing rate in SCN neurons observed following acute melatonin treatment (22). This effect is limited to temporally sensitive times of day. In rat SCN neurons, the highest percentage of SCN cells shows acute alterations in firing rate to melatonin between CT 12 and CT 15 (37). This early night period corresponds to the time when melatonin production by the pineal begins to rise, thus suggesting that the MT_1 receptor could play a role in altering the state of excitability of SCN neurons as the clock moves from day into night. By shifting the membranes to a more hyperpolarized state, it could gate other signals that might impinge concurrently on or within the SCN.

Activation of the MT_2 melatonin receptor, on the other hand, affects clock phasing at dusk and dawn; these are times when endogenous melatonin production is low or nil. As night length increases in the fall, melatonin production expands into this clock phase. Thus perhaps MT_2 melatonin receptor activation communicates information to the clock mechanisms concerning melatonin synthesized during long nights. The MT_2 melatonin receptor may be of critical importance to maintain synchrony of photoperiodic responses under conditions of short photoperiod and also to modify clock responsiveness to other neurochemical regulators of clock phase during the dusk and dawn periods (15). In summary, these two melatonin receptors, MT_1 and MT_2, could provide integrated control of distinct as-

pects of SCN physiology by melatonin and insure that this hormonal signal of darkness within the organism provides an unambiguous message within the range of clock processes.

We are grateful to Monica I. Masana for invaluable help with data analysis. Many thanks go to Shelley Tischkau, Hasanthi Reynolds, and Kathryn Helmin for help with tissue collection. A. E. Hunt contributed the functional studies, and W. M. Al-Ghoul contributed the in situ hybridization and receptor autoradiography studies.

This study was supported by National Institutes of Health Grants NS-22155 (to M. U. Gillette), MH-52685 (to M. L. Dubocovich), and T32-ES-07124 (to W. M. Al-Ghoul).

REFERENCES

1. **Al-Ghoul WM, Herman MD, and Dubocovich ML.** Melatonin receptor subtype expression in human cerebellum. *Neuroreport* 9: 4063–4068, 1998.
2. **Altschul SF, Madden TL, Schaffer AA, Zhang J, Zhang Z, Miller W, and Lipman DJ.** Gapped BLAST and PSI-BLAST: a new generation of protein database search programs. *Nucleic Acids Res* 25: 3389–3402, 1997.
3. **Armstrong SM and Redman JR.** Melatonin and circadian rhythmicity. In: *Melatonin: Biosynthesis, Physiological Effects and Clinical Applications*, edited by Yu HS and Reiter RJ. Boca Raton, FL: CRC, 1993, p. 187–224.
4. **Benloucif S and Dubocovich ML.** Melatonin and light induce phase shifts of circadian activity rhythms in the C3H/HeN mouse. *J Biol Rhythms* 11: 113–125, 1996.
5. **Benloucif S, Masana MI, Yun K, and Dubocovich ML.** Interactions between light and melatonin on the circadian clock of mice. *J Biol Rhythms* 14: 281–289, 1999.
6. **Beresford IJM, North PC, Oakley NR, Starkey S, Brown J, Ford SM, Andrews J, Coughlan J, Stratton S, Dubocovich ML, and Hagan RM.** A non-indolic agonist at high affinity melatonin receptors. *J Pharmacol Exp Ther* 285: 1239–1245, 1998.
7. **Bradford MM.** A rapid and sensitive method for the quantitation of microgram quantities of protein utilizing the principle of protein-dye binding. *Anal Biochem* 72: 248–254, 1976.
8. **Bucher B, Gauer F, Pevet P, and Masson-Pevet M.** Vasoconstrictor effects of various melatonin analogs on the rat tail artery in the presence of phenylephrine. *J Cardiovasc Pharmacol* 33: 316–322, 1999.
9. **Doolen S, Krause DN, Dubocovich ML, and Duckles SP.** Melatonin mediates two distinct responses in vascular smooth muscle. *Eur J Pharmacol* 345: 67–69, 1998.
10. **Dubocovich ML.** Melatonin receptors: are there multiple subtypes? *Trends Pharmacol Sci* 16: 50–56, 1995.
11. **Dubocovich ML, Cardinali DP, Guardiola-Lemaitre B, Hagan RM, Krause DN, Sugden D, Yocca FD, and Vanhoutte PM.** Melatonin receptors. In: *The IUPHAR Compendium of Receptor Characterization and Classification*, edited by Girdlestone D. London: IUPHAR Media, 1998a.
12. **Dubocovich ML and Masana MI.** The efficacy of melatonin receptor analogues is dependent on the level of human melatonin receptor subtype. In: *Biological Clocks, Mechanisms and Applications*, edited by Touitou Y. Amsterdam: Elsevier, 1998, p. 289–293.
13. **Dubocovich ML, Masana MI, Iacob S, and Sauri DM.** Melatonin receptor antagonists that differentiate between the human Mel_{1a} and Mel_{1b} recombinant subtypes are used to assess the pharmacological profile of the rabbit retina ML_1 presynaptic heteroreceptor. *Naunyn Schmiedebergs Arch Pharmacol* 355: 365–375, 1997.
14. **Dubocovich ML, Yun K, Al-Ghoul WM, Benloucif S, and Masana MI.** Selective MT_2 melatonin receptor antagonists block melatonin-mediated phase advances of circadian rhythms. *FASEB J* 12: 1211–1220, 1998.
15. **Gillette MU.** Regulation of entrainment pathways by the suprachiasmatic circadian clock: sensitivities to second messengers. In: *Hypothalamic Integration of Circadian Rhythms, Progress in Brain Research*, edited by Buijs R, Romjin H, Pennartz C, and Mirmiran M. Amsterdam: Elsevier, 1996, vol. 111, p. 119–130.
16. **Gillette MU and McArthur AJ.** Circadian actions of melatonin at the suprachiasmatic nucleus. *Behav Brain Res* 73: 135–139, 1996.
17. **Gillette MU and Tischkau SA.** Suprachiasmatic nucleus: the brain's circadian clock. *Recent Prog Horm Res* 54: 33–58, 1999.
18. **Godson C and Reppert SM.** The Mel_{1a} melatonin receptor is coupled to parallel signal transduction pathways. *Endocrinology* 138: 397–404, 1997.
19. **Guardiola-Lemaitre B.** Melatonin agonist/antagonist: from the receptor to therapeutic applications. In: *Advances in Pineal Research*, edited by Moller M and Pevet P. London: Libbey, 1994, p. 333–348.
20. **Hatton GI, Doran AD, Salm AK, and Tweedle CD.** Brain slice preparation: hypothalamus. *Brain Res Bull* 5: 405–414, 1980.
21. **Lewy AJ, Ahmed S, Jackson JM, and Sack RL.** Melatonin shifts human circadian rhythms according to a phase-response curve. *Chronobiol Int* 9: 380–392, 1992.
22. **Liu C, Weaver DR, Jin X, Shearman LP, Pieschl RL, Gribkoff VK, and Reppert SM.** Molecular dissection of two distinct actions of melatonin on the suprachiasmatic circadian clock. *Neuron* 19: 91–102, 1997.
23. **McArthur JJ, Gillette MU, and Prosser RA.** Melatonin directly resets the rat suprachiasmatic circadian clock in vitro. *Brain Res* 565: 158–161, 1991.
24. **McArthur JJ, Hunt AE, and Gillette MU.** Melatonin action and signal transduction in the rat suprachiasmatic circadian clock: activation of protein kinase C at dusk and dawn. *Endocrinology* 138: 627–634, 1997.
25. **Medanic M and Gillette MU.** Serotonin regulates the phase of the rat suprachiasmatic circadian pacemaker in vitro only during the subjective day. *J Physiol (Lond)* 450: 629–642, 1992.
26. **Miller JA and Zahniser NR.** The use of ^{14}C-labeled tissue paste standards for the calibration of ^{125}I-labeled ligands in quantitative autoradiography. *Neurosci Lett* 81: 345–350, 1987.
27. **Miranda RC and Toran-Allerand CD.** Developmental expression of estrogen receptor mRNA in the rat cerebral cortex: a nonisotopic in situ hybridization histochemistry study. *Cereb Cortex* 2: 1–15, 1992.
28. **Moore RY.** Organization of the mammalian circadian system. In: *Circadian Clocks and Their Adjustment*, edited by Chadwick DJ and Ackrill K. New York: Wiley, 1995, p. 88–106. (Ciba Foundation Symp., London 1993)
29. **Nonno R, Pannacci M, Lucini V, Angeloni D, Fraschini F, and Stankov BM.** Ligand efficacy and potency at recombinant human MT_2 melatonin receptors: evidence for agonist activity of some mt1 antagonists. *Br J Pharmacol* 127: 1288–1294, 1999.
30. **Prosser RA and Gillette MU.** The mammalian circadian clock in the suprachiasmatic nucleus is reset in vitro by cAMP. *J Neurosci* 9: 1073–1081, 1989.
31. **Redman J and Armstrong S.** Free-running activity rhythms in the rat: entrainment by melatonin. *Science* 219: 1089–1091, 1983.
32. **Reppert SM, Godson C, Mahle CD, Weaver DR, Slaugenhaupt SA, and Gusella JF.** Molecular characterization of a second melatonin receptor expressed in human retina and brain: the Mel_{1b} melatonin receptor. *Proc Natl Acad Sci USA* 92: 8734–8738, 1995.
33. **Reppert SM, Weaver DR, and Ebisawa T.** Cloning and characterization of a mammalian melatonin receptor that mediates reproductive and circadian responses. *Neuron* 13: 1177–1185, 1994.
34. **Siuciak JA, Krause DN, and Dubocovich ML.** Quantitative pharmacological analysis of 2-^{125}I-iodomelatonin binding sites in discrete areas of the chicken brain. *J Neurosci* 11: 2855–2864, 1991.
35. **Slaugenhaupt SA, Roca AL, Liebert CB, Altherr MR, Gusella JF, and Reppert SM.** Mapping of the gene for the Mel_{1a}-melatonin receptor to human chromosome 4 (MTNR1A) and mouse chromosome 8 ($Mtnr_{1a}$). *Genomics* 27: 355–357, 1995.

36. **Starkey SJ, Walker MP, Beresford IJM, and Hagan RM.** Modulation of the rat suprachiasmatic circadian clock by melatonin in vitro. *Neuroreport* 6: 1947–1951, 1995.
37. **Stehle J, Vanecek J, and Vollrath L.** Effects of melatonin on spontaneous electrical activity of neurons in the rat suprachiasmatic nuclei: an in vitro iontophoretic study. *J Neural Transm* 78: 173–177, 1989.
38. **Sugden D, McArthur AJ, Ajppru S, Dunie K, and Piggins HD.** Expression of mt(1) receptor subtype mRNA in the entrained rat suprachiasmatic nucleus: a quantitative RT-PCR study across the diurnal cycle. *Brain Res Mol Brain Res* 72: 176–182, 1999.
39. **Sugden D, Yeh LK, and Teh MT.** Design of subtype selective melatonin receptor agonists and antagonists. *Reprod Nutr Dev* 39: 335–344, 1999.
40. **Ting KN, Blaylock NA, and Sugden D.** Molecular and pharmacological evidence for MT_1 melatonin receptor subtype in tail artery of juvenile Wistar rats. *Br J Pharmacol* 127: 987–995, 1999.
41. **Vanecek J.** Cellular mechanisms of melatonin action. *Physiol Rev* 78: 687–721, 1998.
42. **Weaver DR, Liu C, and Reppert SM.** Nature's knockout: the Mel_{1b} receptor is not necessary for reproductive and circadian responses to melatonin in Siberian hamsters. *Mol Endocrinol* 10: 1478–1487, 1996.